



Magnetoresistance scaling in the layered cobaltate $\text{Ca}_3\text{Co}_4\text{O}_9$

P. Limelette, J. C Soret, H. Muguerra, D. Grebille

► To cite this version:

P. Limelette, J. C Soret, H. Muguerra, D. Grebille. Magnetoresistance scaling in the layered cobaltate $\text{Ca}_3\text{Co}_4\text{O}_9$. Physical Review B: Condensed Matter and Materials Physics (1998-2015), 2008, 77 (24), 10.1103/PhysRevB.77.245123 . hal-01870078

HAL Id: hal-01870078

<https://univ-tours.hal.science/hal-01870078>

Submitted on 7 Sep 2018

HAL is a multi-disciplinary open access archive for the deposit and dissemination of scientific research documents, whether they are published or not. The documents may come from teaching and research institutions in France or abroad, or from public or private research centers.

L'archive ouverte pluridisciplinaire **HAL**, est destinée au dépôt et à la diffusion de documents scientifiques de niveau recherche, publiés ou non, émanant des établissements d'enseignement et de recherche français ou étrangers, des laboratoires publics ou privés.

Magnetoresistance scaling in the layered cobaltate $\text{Ca}_3\text{Co}_4\text{O}_9$

P. Limelette,¹ J. C. Soret,¹ H. Muguerra,² and D. Grebille²

¹Laboratoire LEMA, UMR 6157 CNRS-CEA, Université F. Rabelais, UFR Sciences, Parc de Grandmont, 37200 Tours, France

²Laboratoire CRISMAT, UMR 6508 CNRS-ENSICAEN, Université de Caen, 6, Boulevard du Maréchal Juin, 14050 CAEN Cedex, France

(Received 31 March 2008; revised manuscript received 28 May 2008; published 18 June 2008)

We investigate the low-temperature magnetic-field dependences of both the resistivity and the magnetization in the misfit cobaltate $\text{Ca}_3\text{Co}_4\text{O}_9$ from 60 K down to 2 K. The measured negative magnetoresistance reveals a scaling behavior with the magnetization which demonstrates a spin dependent scattering mechanism. This scaling is also found to be consistent with a shadowed metalliclike conduction over the whole temperature range. By explaining the observed transport crossover, this result sheds a new light on the nature of the elementary excitations relevant to the transport.

DOI: 10.1103/PhysRevB.77.245123

PACS number(s): 72.15.Jf, 71.27.+a, 72.25.-b

I. INTRODUCTION

Since correlated oxides as the superconducting cuprates or the manganites with their colossal magnetoresistance^{1,2} have exhibited outstanding properties, the physics of strongly correlated electron materials has motivated an extensive research including both experimental and theoretical investigations.^{1,3} The hunt for new materials has led to the discovery of the layered cobaltates, with striking properties,⁴ a rich phase diagram⁵ including superconductivity⁶ and both metalliclike and insulatinglike characteristics. These compounds being composed of triangular sheets of cobalt atoms share in common with the high-temperature superconductor cuprates the fascinating physics combining the strong correlations and the geometrical frustration in two dimension.⁷

Also, most of the cobaltates display at room temperature a metallic resistivity and a large thermopower allowing for thermoelectric applications. While it is known that either the entropy of localized spins^{8,9} or the electronic correlations¹⁰ can increase thermopower, it has been suggested despite their antagonism that both of them seem to contribute in cobaltates.¹¹ The latter interpretation being still highly debated, the interplay between magnetism and transport properties appears as a very challenging issue to understand the underlying physics in the cobaltates.¹²

In addition, various misfit cobaltates exhibit complex transport properties as metal-insulator crossover and large negative magnetoresistance^{9,13,14} which raise the question of the nature of the elementary excitations. In this context, we report in this paper an experimental study of the single-crystal magnetoresistance and magnetization in the misfit cobaltate $\text{Ca}_3\text{Co}_4\text{O}_9$ in order to connect both of them and to discuss its metallicity.

The studied single crystals were grown using a standard flux method,¹⁵ with typical sizes of the order of $4 \times 2 \times 0.02$ mm³. Similarly to Na_xCoO_2 ,⁴ the structure of the incommensurate cobaltate $[\text{CoCa}_2\text{O}_3]_{0.62}^{\text{RS}}\text{CoO}_2$ (abbreviated hereafter as CaCoO) contains a single $[\text{CoO}_2]$ layer of CdI_2 type stacked with rocksalt-type layers labeled RS instead of a sodium deficient layer. One of the in-plane sublattice parameters being different from one layer to the other,¹³ the cobaltate CaCoO has a misfit structure as in most related compounds.⁹

II. MEASUREMENTS

As frequently observed in misfit cobaltates,^{9,13,14} the temperature dependence of resistivity displayed in Fig. 1 exhibits a transport crossover from a high-temperature metalliclike regime to a low-temperature insulatinglike behavior below nearly 70 K.

Beyond this crossover, two interesting features are worth noting. First, the values of the resistivity remain on the order of the Mott limit¹⁶ over the whole temperature range, i.e., nearly 3 mΩ cm in this compound. This means that the electronic mean-free path is on the order of the magnitude of the interatomic spacing as in a bad metal in the vicinity of a Mott metal-insulator transition^{3,17}, for example. Also, by showing a large negative magnetoresistance, the low-temperature insulatinglike behavior in Fig. 1 tends to be suppressed by the application of a magnetic field. As a consequence of the two previous characteristics, the latter regime does not seem to result from a gap opening in the one-particle electronic spectrum. As a matter of fact, by assuming that the resistivity follows an activated behavior within the temperature range from 30 K up to 80 K as it has earlier been

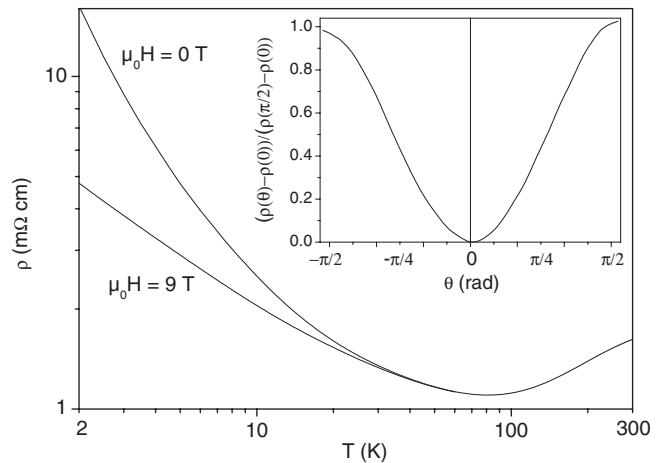


FIG. 1. Temperature dependences of the single crystal in-plane resistivity ρ at 0 T and 9 T, the magnetic field being parallel to the CoO_2 planes. The inset displays the variation of the normalized magnetoresistance with the angle between the CoO_2 planes and the 9 T magnetic field at $T=60$ K.

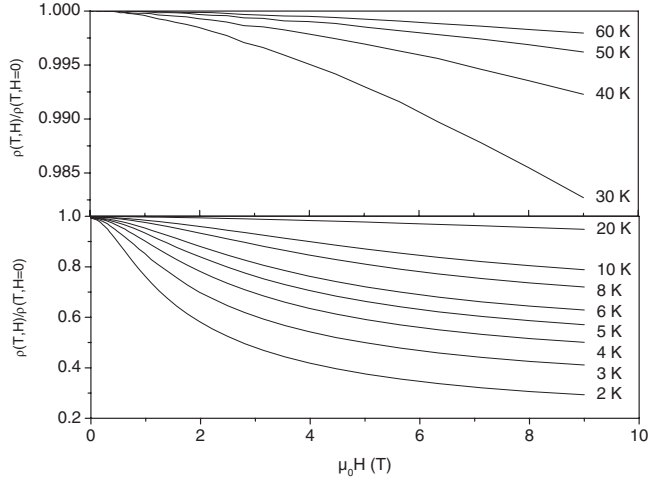


FIG. 2. The upper and lower panels display the magnetic field dependences of the normalized resistivity $\rho(T,H)$ over the whole investigated temperature range, the magnetic field being parallel to the CoO_2 planes.

proposed,¹⁸ the activation energy is found to be lower than the temperature and thus, it results that this energy cannot be related to a gap. In addition, we emphasize that the latter low value leads to unrealistic Coulomb interaction energy¹⁹ which also invalidates such a scenario. Then, in order to investigate this particular low-temperature regime, we have performed both magnetoresistance and magnetization measurements in CaCoO .

A. Magnetoresistance

First, we have measured the single-crystal in-plane resistivity $\rho(H,T)$ using a standard four terminal method at constant temperature T as a function of an in-plane magnetic field $\mu_0 H$, for which the negative magnetoresistance displayed in the inset of Fig. 1 is the largest.

The data reported in Fig. 2 spans the T range from 60 K down to 2 K with a large negative magnetoresistance reaching at the lowest temperature 70% at 9 T.

B. Magnetization

Also, the single-crystal in-plane first magnetization has been measured using a magnetometer of a Quantum Design physical property measurement system on a sample of 3.2 mg. In order to be able to compare these results with the magnetoresistance, the data set reported in Fig. 3 has been measured by applying an in-plane magnetic field.

As it is suggested in Fig. 3 by the sizeable increase in the first magnetization below nearly 20 K a magnetic ordering, already interpreted as a ferrimagnetic transition,¹⁸ occurs within this temperature range. Although it is not displayed in Fig. 3, we emphasize that hysteretic behavior has been observed below 20 K in agreement with the previously reported results.¹⁸

III. SCALING ANALYSIS

A. Low-temperature regime

Thus, let us first focus on the low temperatures data, namely below 20 K. In this temperature range, Fig. 4 dem-

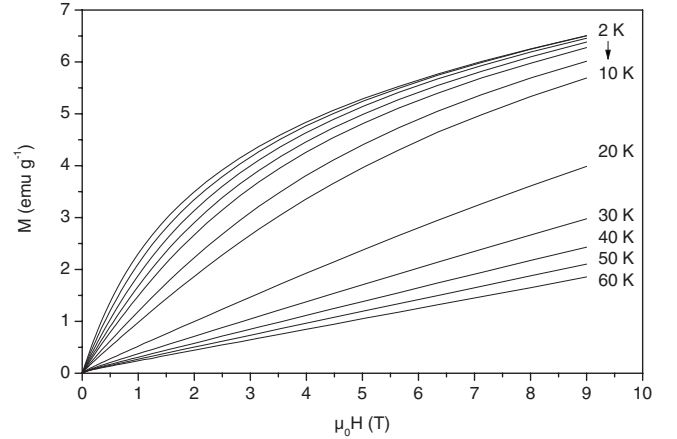


FIG. 3. Magnetic field dependence of the single crystal in-plane magnetization up to 9 T over the whole temperature range, the magnetic field being parallel to the CoO_2 planes.

onstrates that the magnetoresistance fully scales with the magnetization according to an activated form which can be written following Eq. (1),

$$\rho(T,H) = \rho(T,H=0) \exp\left(-\alpha \frac{M^\mu}{T}\right), \quad (1)$$

where α is a constant and the exponent μ equals approximately 2 as expected in the spin dependent transport mechanism proposed by Wagner *et al.*^{20,21} to explain the colossal magnetoresistance measured in the manganites.

This spin dependent transport mechanism is in fact an extension of a variable range hopping^{16,22} to the case of magnetic disorder.^{20,21} The main ideas which underlie this conducting process consist of a variable range spin dependent hopping due to the Hund's coupling $-J_H \cdot \sigma$ between the quasiparticles spin s and the localized spin σ , with the Hund's coupling constant J_H . To basically illustrate this mechanism,

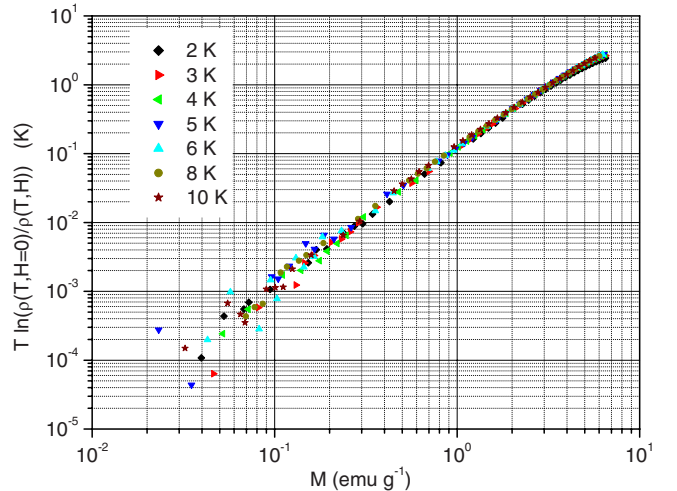


FIG. 4. (Color online) Scaling plot of the single crystal in-plane magnetoresistance as a function of the magnetization at low temperatures.

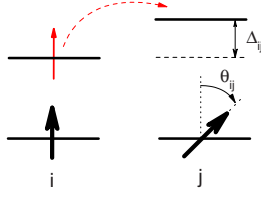


FIG. 5. (Color online) Schematic picture of the electronic energy levels involved in an elementary spin dependent hopping from site i to site j . The magnetic potential barrier Δ_{ij} results from the misorientation θ_{ij} between the quasiparticle spin s_i (thin red arrow) and the localized spin σ_j (bold black arrow) as explained in the text.

let us consider the propagation of a quasiparticle with a spin s_i from site i to site j as sketched in Fig. 5 with the involved spin polarized electronic energy levels.

Because s_i points along the localized spin σ_i direction, the misorientation θ_{ij} between σ_i and the neighbor localized spin σ_j leads to a magnetic potential barrier $\Delta_{ij} = \Delta (1 - \cos \theta_{ij})/2$ with $\Delta = 2J_H s\sigma$. These magnetic potential barriers being distributed over the sample favor a hopping conduction of either activated or variable range hopping (VRH)-type depending on the barriers distribution. Indeed, one might expect an activated conduction if magnetic correlations exist from one site to another (case of a weak magnetic disorder), or a VRH conduction if the paramagnetism persists down to the low temperatures (case of a strong magnetic disorder). Therefore, the reported activated behavior in Fig. 4 seems consistent with the presence of magnetic correlations in this temperature range in agreement with the magnetization data displayed in Fig. 3.

Moreover, the previously mentioned misorientation can be expressed from the local magnetizations $\vec{M}_{i,j}$ at the two sites i and j as $\vec{M}_i \cdot \vec{M}_j = M_S^2 \cos \theta_{ij}$, with the saturation magnetization M_S . It follows that the local magnetic potential barrier is a function of local magnetizations. Then, an applied magnetic field which tends to align the localized spins lowers the magnetic potential barrier and thus implies a negative magnetoresistance as observed in Figs. 1 and 2.

Let us for now discuss the magnetization exponent inferred from the scaling plot in Fig. 4. In the spin dependent transport mechanism proposed by Wagner *et al.*,²⁰ the local magnetizations $M_{i,j}$ are the sum of two different contributions: the Weiss magnetization M_W , which is common to both sites i and j , and the local corrections $\delta M_{i,j}$. The magnetic-field dependent part of the average potential barrier $\langle \Delta_{ij} \rangle$ varying as $\langle \cos \theta_{ij} \rangle$ can then be related to the product $\langle \vec{M}_i \cdot \vec{M}_j \rangle$ and its following expansion:

$$\langle \vec{M}_i \cdot \vec{M}_j \rangle = (M_W)^2 + 2M_W \langle \delta M_i \rangle + \langle \delta M_i \delta M_j \rangle. \quad (2)$$

Three limiting cases can thus occur, involving one of the three terms in the previous relation.

(i) In a paramagnet where $M_W = 0$, the first two terms in Eq. (2) vanish and $\langle \vec{M}_i \cdot \vec{M}_j \rangle$ is expected to scale as the third one, $\langle \delta M_i \delta M_j \rangle = \langle \delta M_i \rangle^2$, namely the square of the paramagnetic magnetization.

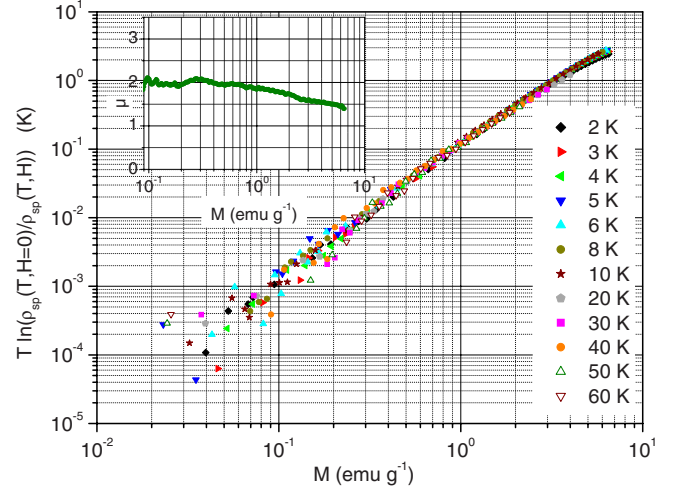


FIG. 6. (Color online) Scaling plot of the effective single crystal in-plane magnetoresistance $\rho_{sp}(T, H)$ as a function of the magnetization over the whole temperature range. Here, $\rho_{sp}(T, H)$ has been calculated by subtracting from the experimental value a constant resistivity at each temperature above 10 K. To make sense, the subtracted part is assumed to be weakly magnetic field dependent. The inset displays the variation of the exponent μ with the magnetization.

In the opposite limit, in a ferromagnetic state with $M_W \gg \langle \delta M_i \rangle$, $\langle \vec{M}_i \cdot \vec{M}_j \rangle$ may be dominated by the first two terms.

(ii) Therefore, if the Weiss magnetization is constant, i.e., both magnetic field and temperature independent (in a high magnetic-field regime), $\langle \vec{M}_i \cdot \vec{M}_j \rangle$ should vary as the second term, namely $\langle \delta M_i \rangle$.

(iii) In a low magnetic-field regime or in a soft ferromagnet, if M_W is both magnetic field and temperature dependent but still higher than $\langle \delta M_i \rangle$, $\langle \vec{M}_i \cdot \vec{M}_j \rangle$ should then scale as the first term, namely M_W^2 .

In particular, cases (i) and (iii) explain why the exponent $\mu=2$ is expected in the low magnetization regime, either correlated or not.

B. High-temperature regime

Furthermore, in order to extend the scaling analysis to higher temperatures, namely above 10 K, let us consider that the resistivity results from two conduction mechanisms. The spin dependent one, ρ_{sp} , gives rise to the observed large negative magnetoresistance whereas the other, ρ_{QP} , is assumed to be weakly magnetic field dependent. Here, the initials QP stand for quasiparticles. According to the Matthiessen rule, the experimental resistivity $\rho(T, H)$ can then be written following Eq. (3),

$$\rho(T, H) \approx \rho_{sp}(T, H) + \rho_{QP}(T). \quad (3)$$

As a matter of fact, if we directly perform the same scaling as in Fig. 4 the data are systematically shifted downward suggesting an incorrect normalization at zero magnetic field and thus, an additional contribution to the resistivity weakly magnetic field dependent.

Therefore, the previous scaling can be extended in Fig. 6

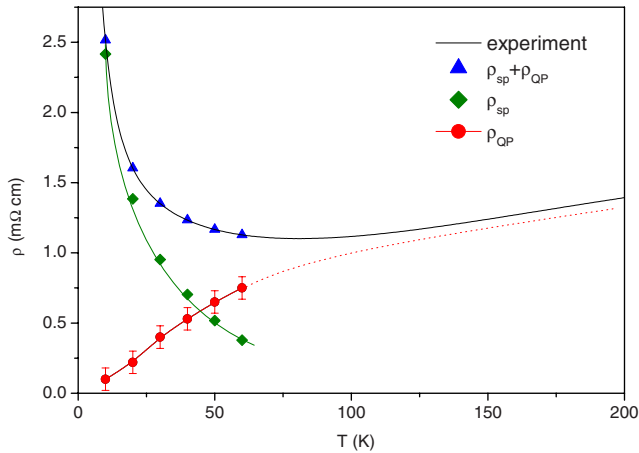


FIG. 7. (Color online). Temperature dependences of the experimental resistivity, the subtracted metalliclike part ρ_{QP} and the deduced insulatinglike part ρ_{sp} . The dotted line is an extrapolation to recover the high-temperature metalliclike behavior.

over the whole temperature range by subtracting the contribution ρ_{QP} to the experimental resistivity up to 60 K, ρ_{QP} being considered as a free parameter. Also, the inset of Fig. 6 displays that the exponent μ equals 2 in the low magnetization regime, either correlated [case (iii)] or not [case (i)], and seems to slightly decrease above $M \approx 1$ emu g^{-1} as suggested in case (ii).

Interestingly, the T dependence of the contribution ρ_{QP} reveals in Fig. 7 a continuous metalliclike behavior down to the low temperatures. Since the metallic part of the magnetoresistance is usually very weak, the found component agrees with the initial assumption of an additional contribution weakly magnetic field dependent.

Besides, both the T dependence and the order of magnitude of ρ_{QP} are consistent with the metalliclike high-temperature regime. As a result, the transport crossover around 70 K appears more as the temperature below which a scattering mechanism predominates over the other rather than a consequence of a qualitative evolution of the system.

In other words, the electronic transport seems to originate from metallic or quasi-metallic conduction over the whole temperature range but shadowed at low temperatures by an efficient spin dependent scattering mechanism. Further, both experimental and theoretical investigations are now needed in order to understand the influences of the misfit structure as well as the frustration induced by the triangular lattice on this shadow metallicity and its connection with the thermopower.

IV. CONCLUSION

To conclude, we have investigated the low-temperature magnetic-field dependence of both the resistivity and the magnetization in the misfit cobaltate CaCoO from 60 K down to 2 K. The measured negative magnetoresistance reveals a scaling behavior with the magnetization which demonstrates a spin dependent scattering mechanism in addition to a shadowed metalliclike conduction over the whole temperature range. This result provides a natural explanation of the observed transport crossover and sheds a new light on the nature of the elementary excitations relevant to the transport.

ACKNOWLEDGMENTS

It is a pleasure to acknowledge useful discussions with S. Hébert, R. Frésard, and Ch. Simon.

- ¹M. Imada, A. Fujimori, and Y. Tokura, *Rev. Mod. Phys.* **70**, 1039 (1998).
- ²M. B. Salamon and M. Jaime, *Rev. Mod. Phys.* **73**, 583 (2001).
- ³A. Georges, G. Kotliar, W. Krauth, and M. J. Rozenberg, *Rev. Mod. Phys.* **68**, 13 (1996).
- ⁴I. Terasaki, Y. Sasago, and K. Uchinokura, *Phys. Rev. B* **56**, R12685 (1997).
- ⁵M. L. Foo, Y. Wang, S. Watauchi, H. W. Zandbergen, T. He, R. J. Cava, and N. P. Ong, *Phys. Rev. Lett.* **92**, 247001 (2004).
- ⁶K. Takada, H. Sakurai, E. Takayama-Muromachi, F. Izumi, R. Dilanian, and T. Sasaki, *Nature (London)* **422**, 53 (2003).
- ⁷J. O. Haerter, M. R. Peterson, and B. S. Shastry, *Phys. Rev. Lett.* **97**, 226402 (2006); C. A. Marianetti and G. Kotliar, *ibid.* **98**, 176405 (2007); A. H. Nevidomskyy, C. Scheiber, D. Sénéchal, and A.-M. S. Tremblay, *Phys. Rev. B* **77**, 064427 (2008).
- ⁸W. Koshibae, K. Tsutsui, and S. Maekawa, *Phys. Rev. B* **62**, 6869 (2000); K. Koumoto, I. Terasaki, and M. Murayama, *Oxide Thermoelectrics* (Research Signpost, India, 2002); Y. Wang, N. Rogado, R. Cava, and N. Ong, *Nature (London)* **423**, 425 (2003).
- ⁹A. Maignan, S. Hébert, M. Hervieu, C. Michel, D. Pelloquin, and D. Khomskii, *J. Phys.: Condens. Matter* **15**, 2711 (2003).

- ¹⁰G. Pálsson and G. Kotliar, *Phys. Rev. Lett.* **80**, 4775 (1998); J. Merino and R. H. McKenzie, *Phys. Rev. B* **61**, 7996 (2000); K. Behnia, D. Jaccard, and J. Flouquet, *J. Phys.: Condens. Matter* **16**, 5187 (2004); O. I. Motrunich and P. A. Lee, *Phys. Rev. B* **69**, 214516 (2004); P. Limelette, V. Hardy, P. Auban-Senzier, D. Jérôme, D. Flahaut, S. Hébert, R. Frésard, C. Simon, J. Noudem, and A. Maignan, *ibid.* **71**, 233108 (2005).
- ¹¹P. Limelette, S. Hébert, V. Hardy, R. Frésard, C. Simon, and A. Maignan, *Phys. Rev. Lett.* **97**, 046601 (2006).
- ¹²H. J. Xiang and D. J. Singh, *Phys. Rev. B* **76**, 195111 (2007); J. Bobroff, S. Hébert, G. Lang, P. Mendels, D. Pelloquin, and A. Maignan, *ibid.* **76**, 100407(R) (2007).
- ¹³A. C. Masset, C. Michel, A. Maignan, M. Hervieu, O. Toulemonde, F. Studer, B. Raveau, and J. Hejtmanek, *Phys. Rev. B* **62**, 166 (2000).
- ¹⁴T. Yamamoto, K. Uchinokura, and I. Tsukada, *Phys. Rev. B* **65**, 184434 (2002).
- ¹⁵C. Xia, J. Sugiyama, H. Itahara, and T. Tani, *J. Cryst. Growth* **276**, 519 (2005).
- ¹⁶N. F. Mott and E. A. Davis, *Electronic Processes in Non Crystalline Materials* (Clarendon, Oxford, 1979).
- ¹⁷P. Limelette, P. Wzietek, S. Florens, A. Georges, T. A. Costi,

- C. Pasquier, D. Jérôme, C. Mézière, and P. Batail, Phys. Rev. Lett. **91**, 016401 (2003).
- ¹⁸J. Sugiyama, H. Itahara, T. Tani, J. H. Brewer, and E. J. Ansaldo, Phys. Rev. B **66**, 134413 (2002).
- ¹⁹D. J. Singh, Phys. Rev. B **61**, 13397 (2000).
- ²⁰P. Wagner, I. Gordon, L. Trappeniers, J. Vanacken, F. Herlach, V. V. Moshchalkov, and Y. Bruynseraede, Phys. Rev. Lett. **81**, 3980 (1998).
- ²¹M. Viret, L. Ranno, and J. M. D. Coey, Phys. Rev. B **55**, 8067 (1997).
- ²²A. L. Efros and B. L. Shklovskii, J. Phys. C **8**, L49 (1975).